

# Knitted silk mesh-like scaffold incorporated with sponge-like regenerated silk fibroin/collagen I and seeded with mesenchymal stem cells for repairing Achilles tendon in rabbits

LIANG TANG<sup>1</sup>, YADONG YANG<sup>2</sup>, YUEZHONG LI<sup>1</sup>, GENG YANG<sup>2</sup>,  
TAO LUO<sup>2</sup>, YIMENG XU<sup>2</sup>, WENYUAN ZHANG<sup>2\*</sup>

<sup>1</sup> Institute of Health Food, Zhejiang Academy of Medical Sciences, Hangzhou, Zhejiang Province, China.

<sup>2</sup> Institute of Bioengineering, Zhejiang Academy of Medical Sciences, Hangzhou, Zhejiang Province, China.

A scaffold knit with natural sericin-free silk fibroin fiber possesses desirable mechanical properties, biocompatibility, ease of fabrication, and slow degradability. However, regenerated silk fibroin degrades faster than natural silk. In this study, natural silk fibroin fiber mesh-like scaffolds were prepared by a weft-knitting method and the pores were filled with sponge-like regenerated silk fibroin-collagen I. The microporous sponge and mesh-like scaffolds were fused to achieve gradient degradation of the scaffolds, and rabbit bone marrow mesenchymal stem cells (BMSCs) were seeded onto the scaffolds to form scaffold-BMSCs composites. The composites were implanted into gap defects made in the rabbit Achilles tendon. Twenty weeks after implantation, histological observation showed that tendon-like tissue had formed, collagen I mRNA was expressed, abundant collagen was generated, and that there was no obvious degradation of silk. The maximum load of the neo-Achilles tendon was 62.14% that of the natural Achilles tendon. These outcomes were superior to those obtained in the group implanted with a scaffold without BMSCs. These findings suggest the feasibility of constructing tissue-engineered tendons using weft-knitted silk scaffolds incorporated with sponge-like regenerated silk fibroin/collagen I and seeded with BMSCs, and show potential of the scaffold-BMSCs composites to repair Achilles tendon defects.

*Key words: Bombyx mori silk, regenerated silk fibroin, collagen I, bone marrow-derived mesenchymal stem cells, weft-knit, Achilles tendon action*

## 1. Introduction

Tendon injury is one of the most common sports injuries and a well-recognized treatment problem in orthopedics and sports medicine since the tendon has limited ability to self-repair. The repaired tendon is composed of scar tissue with poor tissue structure and mechanical properties which predispose the tendon to recurrent fractures [1]. Each year, nearly 30 million people worldwide receive medical treatment for tendon and ligament injuries [2]. Although there are several different treatment options (i.e., non-surgical, surgical therapeutic approaches, rehabilitation therapy) of

tendon injury, the effectiveness of these traditional treatments remain unsatisfactory. Indeed, the repaired tendon may never return to its pre-injury functional status. Accordingly, the treatment of tendon injury has become an increasingly popular area of research in sports medicine. Traditionally, tendon autografts or allografts were mainly used for the repair of tendon injury. However, the clinical application of tendon autografts is limited because of the low availability of tendons and the resultant dysfunction at the donor site. Similarly, the availability of tendon allografts is also very limited and the procedure is relatively expensive. In addition, there are many risks associated with tendon autografts and allografts, including disease trans-

\* Corresponding author: Wenyuan Zhang, Zhejiang Academy of Medical Sciences, 182 Tian Mu Shan Road, Hangzhou 310013, Zhejiang Province, China, 310013 Hangzhou, China. Phone: 86-571-88215587, e-mail: zhangwy61@163.com

Received: April 4th, 2018

Accepted for publication: August 10th, 2018

mission, immune rejection, and inadequate repair. Alternatively, an artificial tendon prosthesis has short-term biomechanical strength similar to that of the normal tendon, but is associated with a high rate of immune rejection and poor durability issues, and is also degraded slowly and causes infection. With the development of new tissue engineering techniques, research on tissue-engineered tendons has provided new insight for strategies of tendon repair and regeneration [3]. Compared to conventional therapeutic approaches for the repair of tendon injury, application of a tissue-engineered tendon is free of the aforementioned issues associated with tendon autografting or allografting. However, the biomaterials selected for the design of tissue-engineered tendons should be biocompatible; that is, when contacting the body, they should not result in adverse reactions, and they must facilitate cell adherence, induce collagen deposition and promote the generation of new tendon tissue with close-to-normal biomechanical strength. Currently, the most critical limiting factors related to tissue-engineered tendon research are how to obtain a large amount of seed cells with regenerative capacity and to select an ideal scaffold biomaterial with mechanical strength similar to that of the normal human tendon tissue.

Continued research and development on scaffold biomaterials is the key toward realizing successful tissue-engineered tendons because the scaffold biomaterial provides a stable external environment for cell growth. Indeed, seed cells will die if there is no suitable scaffold to provide an appropriate living environment for tendon cells [4]. Accordingly, preparation of three-dimensional biomimetic scaffolds with desirable biocompatibility and mechanical strength is the most urgent problem to resolve in the clinical treatment of tendon injury and for tendon regeneration [5]. An ideal tissue-engineered tendon scaffold should exhibit desirable biocompatibility and bioactivity, mechanical strength similar to that of the natural collagen tissue, a three-dimensional structure, and a water-absorbing property [6]. Tissue-engineered tendons constructed with silk fibroin fibers reportedly provide a unique combination of advantages over conventional artificial tendons [7], [8]. Natural silk fibroin fibers have recently received increased research attention owing to their several beneficial properties, including excellent mechanical strength, biocompatibility, adequate sources of raw materials, desirable processing properties, and plasticity [9]. Therefore, silk fibroin fiber has great potential for clinical applications, and thus development of a silk fibroin fiber-based biomaterial is of great significance for construction of tissue-engineered tendons.

Nevertheless, it is extremely difficult to match the rate of scaffold biomaterial degradation with the rate of tissue formation, which is a critical factor for achieving the appropriate shape and mechanical integrity of a tissue-engineered structure. From this perspective, regenerated silk fibroin degrades faster than natural silk [10]–[12]. Moreover, natural silk scaffolds incorporated with a sponge-like regenerated silk fibroin/collagen could provide sufficient space for cell growth [15]. Collagen would be degraded first, followed by regenerated silk fibroin, and then natural silk fibroin, which would achieve gradient degradation of the silk scaffold. This design provides a new opportunity for the development of a tissue-engineered tendon scaffold.

The architecture of a tendon scaffold should facilitate cell seeding, proliferation, migration, and differentiation, while retaining a certain degree of mechanical strength to collectively contribute to the repair of tendon injury. Altman et al. [9] found that silk fibers twisted into a cable showed strong fatigue resistance, and the mechanical properties of this twisted cable-like scaffold were similar to those of human anterior cruciate ligaments [9], [13], [14]. However, such cable-like scaffolds also have shortcomings. In particular, their internal dense structure makes cell ingrowth very difficult, which would, in turn, hinder the ingrowth of newly generated tissue. Alternatively, a weft-knitted mesh scaffold exhibits sufficient mechanical strength along with excellent flexibility and softness [15], [16], which would facilitate cell seeding and air exchange. Indeed, compared with other types of woven structures, weft-knitted structures can provide more space for tissue ingrowth.

Seed cells and scaffold biomaterials are the major factors contributing to the construction of tissue-engineered tendons and are the keys to the formation of tissue-engineered bioactive tissues. Since tenocytes are the basic functional units of the tendon tissue, they should be the most suitable choice of seed cells. However, there are fewer sources of tenocytes than other cell types. Moreover, tenocytes differentiate into mature functional cells and proliferate slowly and age easily during *in vitro* culture, ultimately losing the ability to proliferate after several passages. In addition, harvesting tenocytes may result in impaired function of the tendon. Bone marrow mesenchymal stem cells (BMSCs) have been recently accepted as ideal seed cells for a tissue-engineered tendon [17], [18] owing to their several advantages. First, harvesting BMSCs causes relatively minor injury to the body. Second, BMSCs are easily isolated and purified, and

they can greatly proliferate after short-term culture with low immunogenicity, differentiate into tenocyte-like cells, survive in the tendon for a long time, promote maturation and healing of the tendon, and increase the mechanical strength of the repaired tendon [18], [19]. Finally, BMSCs, regardless of their quantity or quality, meet the requirement of seed cells used for construction of the tendon tissue [20]. Overall, these properties suggest the feasibility and effectiveness of BMSCs as the seed cells for tendon regeneration [21].

Based on this background, in this study, we prepared silk scaffolds using a weft-knitting method, which were filled with sponge-like regenerated silk fibroin/collagen and seeded with rabbit BMSCs. After 7 days of *in vitro* culture, the composites were implanted into gap defects made in the rabbit Achilles tendon to construct a tissue-engineered tendon. We monitored the ability of the scaffold–BMSCs composites to repair the rabbit Achilles tendon defects under the action of cytokines under *in vivo* environment and stress.

## 2. Materials and methods

### 2.1. Isolation and identification of rabbit BMSCs

Clean female New Zealand rabbits aged 3 months, about 2.2 kg, were supplied by Zhejiang Provincial Experimental Animal Center (Hangzhou, China; certificate No. SCXK (Zhe) 2013-0055).

After anesthesia by injection of 3% sodium pentobarbital (1.1 mL/kg) via the marginal ear veins under aseptic conditions, bone marrow (3 mL) was harvested by puncturing the iliac crest under aseptic conditions. After the addition of 2 mL of heparin-containing culture medium, the harvested bone marrow was transferred into a centrifuge tube containing Percoll solution (1.073 g/mL) and centrifuged at  $800 \times g$  for 20 min. The white layer (containing mononuclear cells) was carefully drawn into another centrifuge tube. After the addition of low-glucose DMEM containing 10% fetal bovine serum (FBS), the resulting preparation was thoroughly mixed, centrifuged, and washed. After 2 weeks of adherent culture, the cells were obtained by isolation and purification. Passage-3 cells were identified using flow cytometry (FACSCalibur, USA) with anti-rabbit CD14-FITC and anti-rabbit CD44-PE (both from Antigenix, USA).

### 2.2. Preparation of weft-knitted silk scaffolds

*Bombyx mori* silk (obtained from Hangzhou silk market, China) was boiled for 30 min in 0.5%  $\text{Na}_2\text{CO}_3$  solution (1 g silk: 1000 mL 0.5%  $\text{Na}_2\text{CO}_3$  solution) and for another 30 min after refreshing the  $\text{Na}_2\text{CO}_3$  solution. After removal of the glue-like sericin proteins of the silk fibers, the silk was rinsed with deionized water at 95 °C and dried at 22–25 °C. Thus, sericin-free silk fibroin fibers were obtained. A total of 360 sericin-free silk fibroin fiber monofilaments (180 monofilaments per strand) were twisted into a small bundle. Then the bundles were weft-knitted into a long mesh-like scaffold ( $43 \times 6$  mm) (Fig. 1). The mesh-like scaffolds were then separately rinsed in 0.1 mol/L HCl, distilled water, and 0.1 mol/L NaOH, and then placed in a distilled water ultrasonic cleaner to get rid of all impurities. One scaffold was gold-sputtered and observed under a scanning electron microscope (SU8010, Hitachi, Japan).

### 2.3. Preparation of the silk fibroin solution

The sericin-free silk fibroin fiber prepared as described in Section 2.2 was cut into small sections and then dissolved in a ternary solvent system of  $\text{CaCl}_2$ :  $\text{H}_2\text{O}$ : $\text{C}_2\text{H}_5\text{OH}$  (1:8:2 molar ratio) at 80 °C and stirred at 600 r/min. After 3 days of dialysis with deionized water, the silk fibroin solution was obtained and prepared into a 2 wt. % silk fibroin solution via concentration for later use.

### 2.4. Preparation of a silk mesh-like scaffold incorporated with a sponge-like regenerated silk fibroin/collagen composite

Rat tail collagen I (0.5 wt%, 5 mg/mL; Hangzhou Shengyou Biotechnology Co., Ltd., China) was neutralized with 0.1 mol/L NaOH and then mixed with an equal volume of the 2 wt% sericin-free silk fibroin solution. The long mesh-like scaffold prepared as described in Section 2.2 was sodden with the resulting product, placed in a refrigerator at –60 °C overnight, lyophilized in a freeze-dryer (Heto PowerDry LL3000, Denmark), and sterilized with ethylene oxide for later use. One scaffold was gold-sprayed and observed under the scanning electron microscope (SEM).

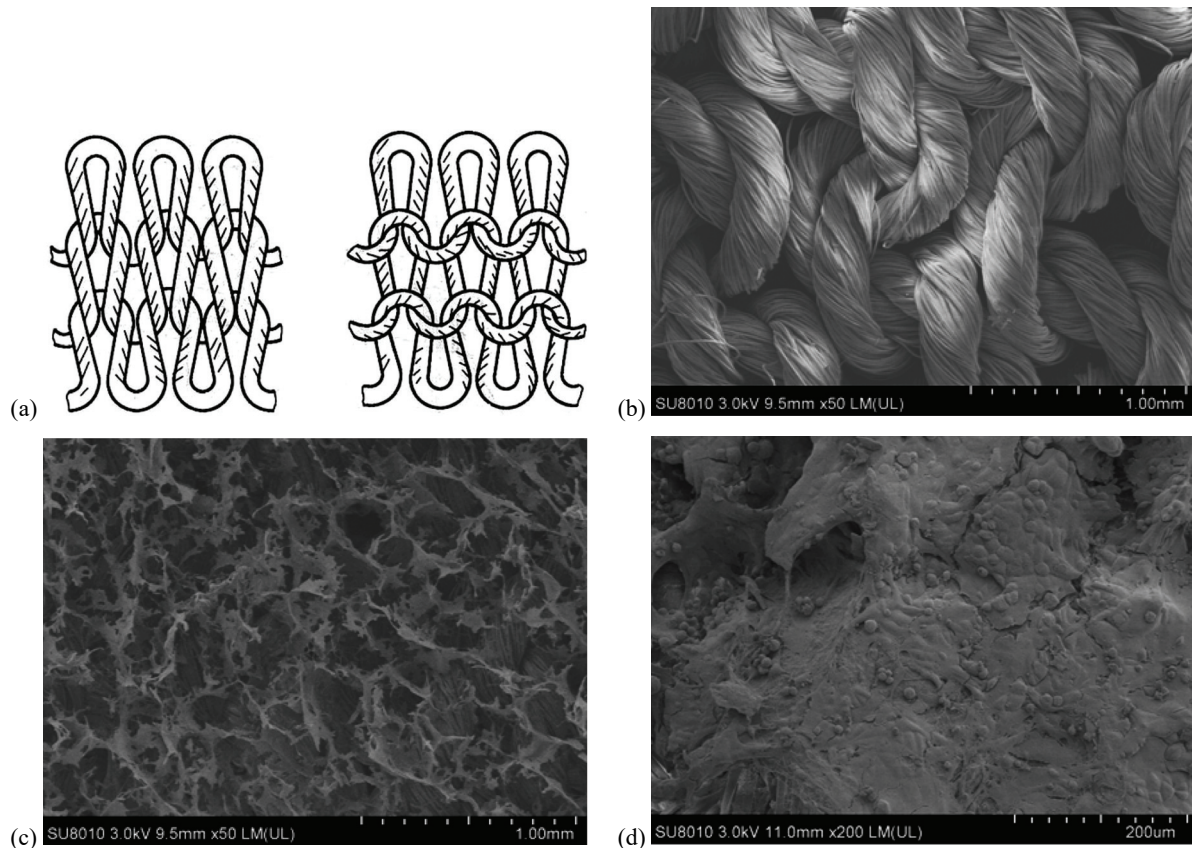


Fig. 1. Weft-knitted silk mesh-like scaffolds incorporated with sponge-like regenerated silk fibroin/collagen I and bone marrow-derived mesenchymal stem cells (BMSCs) growing on the scaffold. (a) Schematic of the weft knitting. Left: front; right: back. (b) Mesh scaffold of weft-knitted silk fibroin fibers ( $\times 50$ ). (c) Weft-knitted silk mesh-like scaffolds incorporated with sponge-like regenerated silk fibroin/collagen I ( $\times 50$ ). (d) Scanning electron microscope image of BMSCs growing on a weft-knitted silk mesh-like scaffold incorporated with sponge-like regenerated silk fibroin/collagen I ( $\times 200$ ). After culture of the composites for 48 h, scanning electron microscopy revealed that the spindle-shaped BMSCs adhered to the scaffold, grew vigorously, and proliferated rapidly on the scaffold

### 2.5. *In vitro* culture of scaffold–BMSCs composites

Fibronectin (Zhengzhou Fuborui Biotechnology Co., Ltd., China) was prepared in a 200  $\mu\text{g}/\text{mL}$  solution using the cell culture medium. The sterilized silk mesh-like scaffold incorporated with sponge-like regenerated silk fibroin/collagen was soaked in the 200  $\mu\text{g}/\text{mL}$  fibronectin solution, left for 24 h at 4  $^{\circ}\text{C}$ , and dried at 22–25  $^{\circ}\text{C}$ . The scaffold was fixed in a U-shaped spring and subjected to a tension of 0.2 N. The suspension of passage-3 BMSCs ( $2 \times 10^7/\text{mL}$ ), at approximately 0.3 mL per scaffold, was injected into the scaffold, so that the cells were sufficiently permeated into the pores of the scaffold. The scaffold was then incubated at 37  $^{\circ}\text{C}$  and 5%  $\text{CO}_2$  for 2 h in a  $\text{CO}_2$  incubator (Thermo Electron Corporation, USA). After addition of a sufficient amount of 10% FBS-containing low-glucose DMEM, the scaffold was *in vitro*-cultured

for additional 7 days. The culture medium was refreshed every other day. Thus, scaffold–BMSCs composites were obtained. The same scaffolds, but without BMSCs, were used as controls. At 48 h of culture, one scaffold–BMSCs composite was observed by scanning electron microscope (SEM) after conventional operating instruction.

### 2.6. Preparation of rabbit models of Achilles tendon defects and implantation of scaffold–BMSCs composites

Twenty-eight rabbits were included in the experimental group. After anesthesia by injection of 3% sodium pentobarbital (1.1 mL/kg) via the marginal ear vein, a 15-mm-long Achilles tendon was excised from a random limb, and thus the Achilles tendon was

automatically retracted, leading to an approximately 26-mm-long gap. The scaffold–BMSCs composite cultured for 7 days *in vitro* was folded in half. After appropriate stretching, a double-layered scaffold–BMSCs composite, approximately 26 mm × 4 mm in size, was created and then implanted into the gap defect in the rabbit Achilles tendon. The double-layered scaffold–BMSCs composite was tightened through tension adjustment and then surgical suturing was performed using the modified Kessler suture procedure. No surgical intervention was applied on the contralateral side. In an additional 28 rabbits, a double-layered scaffold without BMSCs was implanted to bridge the 26-mm-long gap made at a random Achilles tendon, which served as controls. After surgery, the incisions were routinely closed, and penicillin was injected in the abdomen for three successive days at a dose of 500,000 U a day, per animal. These animals were raised in separate cages. The operated limbs were not fixed, and the animals' survival, food intake, and locomotor activity were monitored.

## 2.7. Monitoring of rabbit Achilles tendon repair

At 10 and 20 weeks after surgery, half the animals were randomly sacrificed by an overdose of sodium pentobarbital (55 mg/kg). The repaired Achilles tendon was grossly observed. Subsequently, three newly Achilles tendon specimens from each group were routinely fixed, embedded with paraffin, cross-sectioned, and stained with hematoxylin-eosin and Masson trichrome for histological and scaffold degradation observation. Eight of the neo-Achilles tendon specimens from each group were then selected for mechanical strength measurement. Precisely, the two ends of the neo-Achilles tendon were tightly wrapped with gauze and vertically fixed to the two metal clamps of a mechanical testing machine (QX-W300, Shanghai, China). The distance between the two clamps and the cross-sectional dimensions of the tendon were measured using a Vernier caliper. The specimens were kept moist throughout the measurements. Three pre-tensile strength tests were performed with a designated strength of 5 N. The tensile breaking test with a tensile speed of 30 mm/min was carried out to record the maximum load, maximum stress, and elastic modulus. These indices were compared between operated and normal Achilles tendons (8 randomly selected). Finally, the mRNA expression levels of collagen I and III were determined with quantitative RT-PCR in three specimens from each group. The

middle part of each specimen was used from Achilles tendon tissue blocks. In brief, 20–50 mg of the specimen was washed with phosphate-buffered saline and RNA was extracted using the Ultrapure RNA kit (Beijing Kangwei Century Biotech Co., Ltd., Beijing, China). RNA (0.5 µg) was reverse transcribed, and real-time PCR was conducted using SYBR Green Bestar™ Real Time PCR Master Mix (DBI, Germany) on a Rotor-Gene 3000 real-time PCR instrument (Corbett Research, Germany) according to the manufacturer's instructions. *GAPDH* was employed as an internal reference gene. The primer sequences of collagen I, collagen III, and *GAPDH* were previously reported [15], [22].

## 2.8. Statistical analysis

Data were expressed as the mean ± standard deviation and were analyzed using SPSS 13.0 software. Pairwise comparisons between groups were conducted using *t*-tests.  $P < 0.05$  was considered statistically significant.

# 3. Results

## 3.1. Culture of BMSCs

The mononuclear cell layer was extracted from the bone marrow using density-gradient centrifugation and then cultured. Non-adherent cells were thrown away, refreshing the medium. The remaining adherent cells were the BMSCs. Passage-3 BMSCs were evenly distributed with a spindle-shaped appearance, grew vigorously, and proliferated rapidly (Fig. 2a). Flow cytometry revealed that these cells were negative for CD14 (Fig. 2b) and positive for CD44 (Fig. 2c), confirming the BMSC phenotype.

## 3.2. SEM observation of silk scaffolds incorporated with sponge-like regenerated silk fibroin/collagen and BMSC growth on the scaffold composite

The sericin-free silk fibroin fiber bundle was weft-knitted according as shown in Fig. 1a. The weft-knitted silk mesh-like product is shown in Fig. 1b, and the silk scaffolds incorporated with sponge-like re-

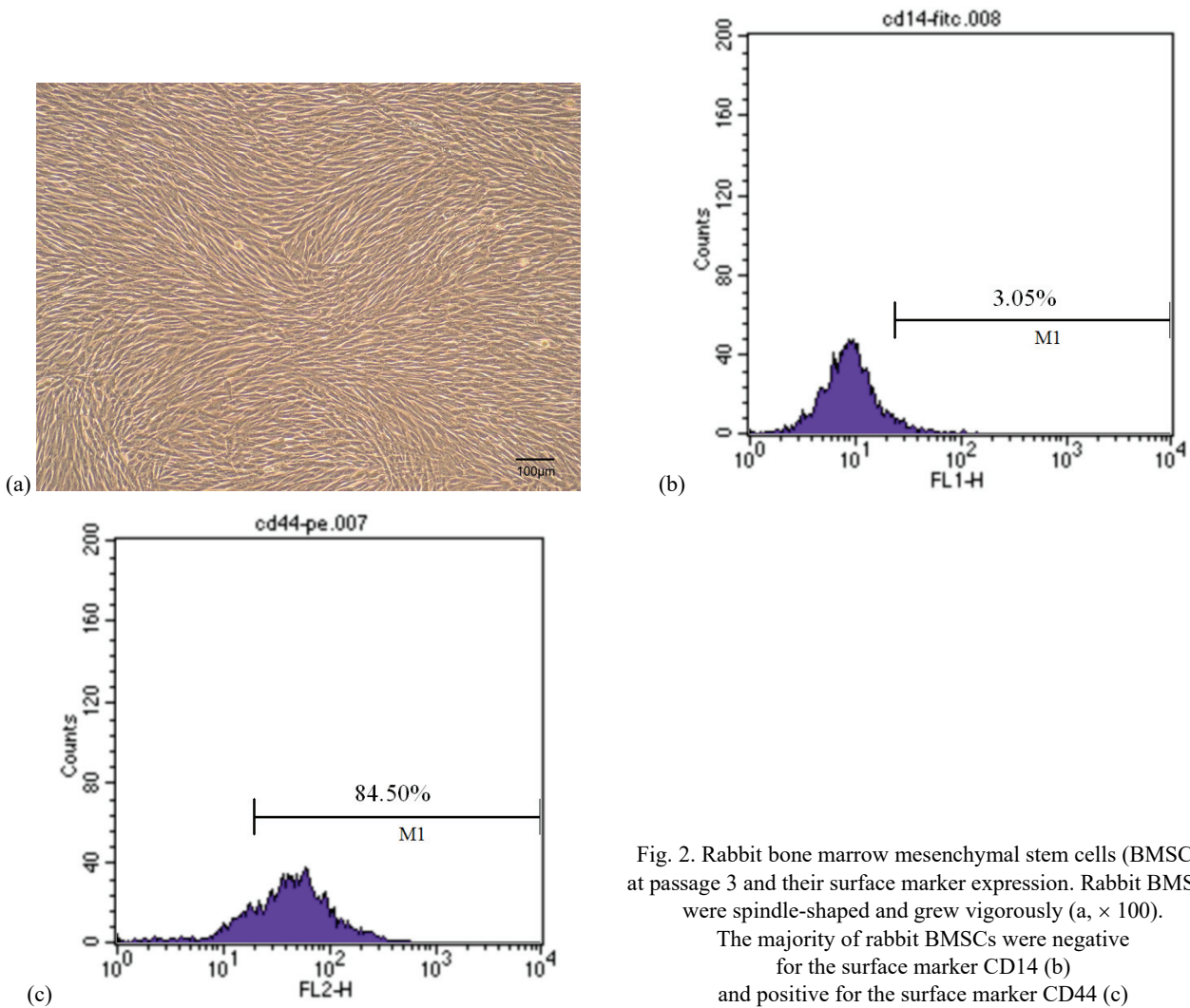


Fig. 2. Rabbit bone marrow mesenchymal stem cells (BMSCs) at passage 3 and their surface marker expression. Rabbit BMSCs were spindle-shaped and grew vigorously (a,  $\times 100$ ). The majority of rabbit BMSCs were negative for the surface marker CD14 (b) and positive for the surface marker CD44 (c)

generated silk fibroin/collagen which were then seeded with BMSCs to obtain the scaffold–BMSCs composites, are shown in Fig. 1c. After culture of the composites for 48 h, scanning electron microscopy revealed that the spindle-shaped BMSCs adhered to the scaffold and grew vigorously (Fig. 1d).

### 3.3. Evaluation of rabbit Achilles tendon repair

#### 3.3.1. Gross observation

After surgery, all animals survived until the end of the experimental period. During the survival period, the animals showed normal food intake, excretion, and locomotor activity. At 1 week post-operatively, muscle redness and swelling occurred in the region around the scaffold implantation site, but no muscle tissue degeneration, necrosis, or infection was observed. At 3 weeks post-operatively, the muscle redness and swelling had

largely subsided. At 10 and 20 weeks after scaffold implantation, the cord-like neo-Achilles tendon-like tissue was visible in the region around the scaffold implantation site. Over time, the neo-Achilles tendon-like tissue gradually changed from a dark red to ivory white color, with significantly improved texture. The color and texture of the neo-Achilles tendon-like tissue in experimental group were superior to those in control group.

#### 3.3.2. Histological observation and scaffold degradation evaluation

At 10 and 20 weeks post-operatively, hematoxylin-eosin staining revealed excellent histocompatibility between the scaffold and peripheral tissue in both the experimental and control groups (Figs. 3a–d). At 20 weeks post-operatively, muscle grew into the silk scaffold, and the neo-Achilles tendon-like tissue grew into the scaffold to form a “reinforced concrete”-like structure (Figs. 3c, d). Compared to the control group,

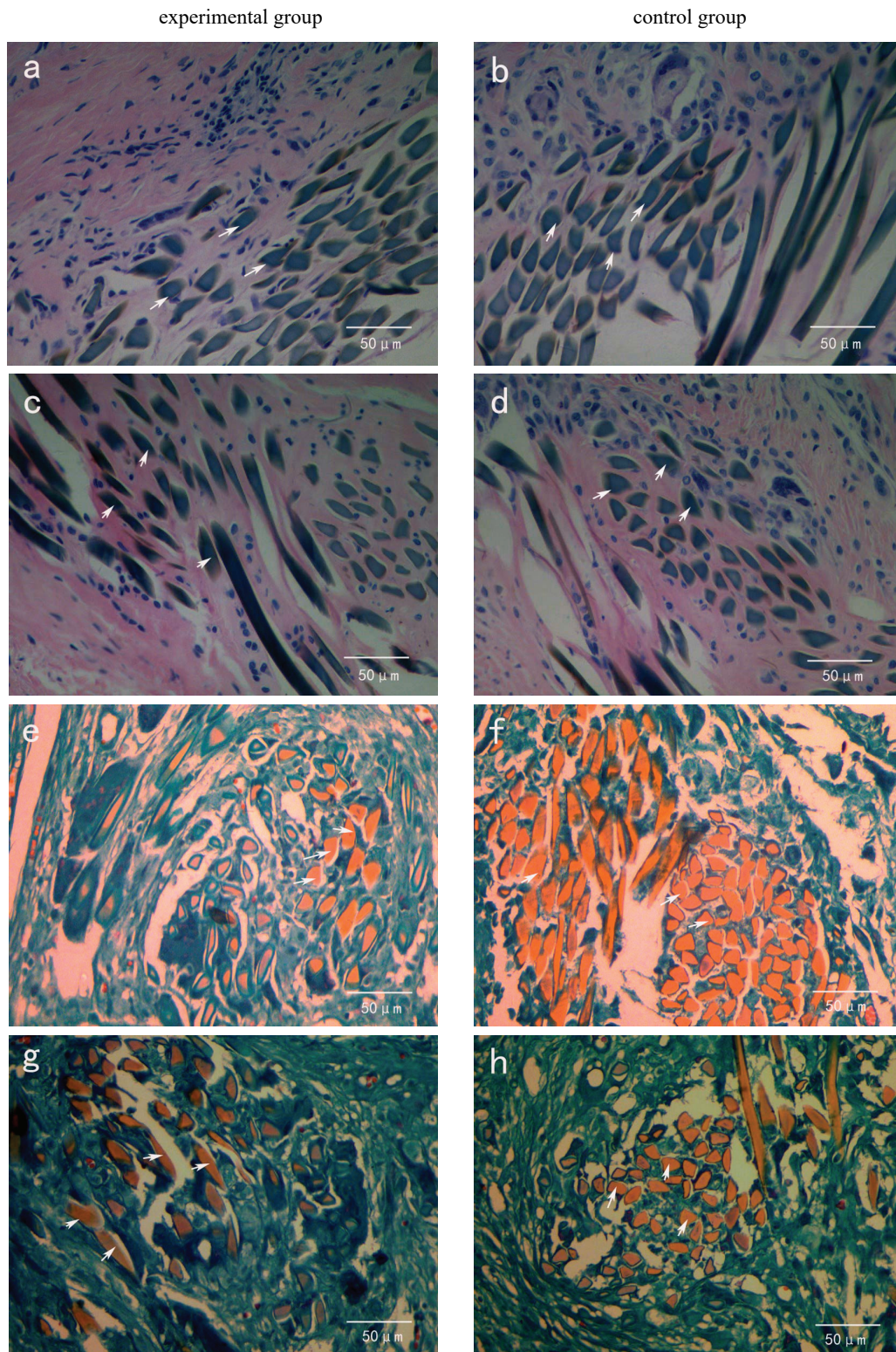


Fig. 3. Histological (a–h,  $\times 400$ ) observation of the neo-Achilles tendon after cross-sectioning. Hematoxylin-eosin (HE) staining results of the experimental (a) and control (b) groups, and Masson trichrome staining of the experimental (e) and control (f) groups at 10 weeks post-operatively. HE staining of the experimental (c) and control (d) groups, and Masson trichrome staining results of the experimental (g) and control (h) groups at 20 weeks post-operatively. At 10 and 20 weeks post-operatively, collagen production and silk fibroin (white arrows) residue were identified in the neo-Achilles tendons of experimental group (a, c, e, g) and control group (b, d, f, h). Neo-Achilles tendon tissues grew into the scaffold to form a “reinforced concrete”-like structure.

Tissues surrounding the neo-tendon were more tightly connected in the experimental group (a, c, e, g) than those in the control group (b, d, f, h). At 10 weeks post-operatively, the silk fibroin fibers were relatively more loosely bound to the new tissues; at 20 weeks post-operatively, connections between the silk fibroin fibers and new tissues became tighter

Table 1. Biomechanical test results in the three groups at 10 and 20 weeks postoperatively ( $n = 8$ , mean  $\pm$  SD)

group	Maximum load [N]		Maximum stress [MPa]		Elastic modulus [MPa]	
	10 weeks	20 weeks	10 weeks	20 weeks	10 weeks	20 weeks
Control	186.33 $\pm$ 33.21	194.28 $\pm$ 37.84	21.27 $\pm$ 3.82	23.75 $\pm$ 4.62	178.15 $\pm$ 32.01	192.43 $\pm$ 36.88
Experimental	199.42 $\pm$ 33.75	232.72 $\pm$ 43.63 <sup>a</sup>	22.89 $\pm$ 3.85	28.27 $\pm$ 5.41 <sup>a</sup>	195.98 $\pm$ 33.24	234.68 $\pm$ 44.32 <sup>a</sup>
Normal Achilles tendon	366.94 $\pm$ 41.28 <sup>bc</sup>	374.53 $\pm$ 45.14 <sup>bc</sup>	39.56 $\pm$ 4.72 <sup>bc</sup>	40.45 $\pm$ 4.83 <sup>bc</sup>	378.27 $\pm$ 46.58 <sup>bc</sup>	389.22 $\pm$ 45.91 <sup>bc</sup>

<sup>a</sup>  $P < 0.05$ , <sup>b</sup>  $P < 0.001$  vs. control group, <sup>c</sup>  $P < 0.001$  vs. experimental group.

a more abundant and tighter matrix was observed in the experimental group. There was no obvious degradation of silk observed in either group (Figs. 3a–h). Masson's trichrome staining (Fig. 3e) revealed that at 10 weeks post-operatively, there was abundant collagen (green staining) in the regenerated tissue in the experimental group. At 20 weeks post-operatively, there was an even larger amount of collagen detected (Fig. 3g). At 10 and 20 weeks after scaffold implantation, the cell arrangement was more disordered, and silk fibroin fibers were relatively more loosely bound to the new tissues in control group (Fig. 3b, d, f, h) than those in experimental group (Figs. 3a, c, e, g). In other words, regardless of the collagen formation, cell arrangement was inferior in control group compared to that in experimental group.

### 3.4. Biomechanical test results of the neo-Achilles tendon

The biomechanical test results of the neo-Achilles tendon-like tissue are shown in Table 1. At 10 and 20 weeks post-operatively, the maximum load of the neo-Achilles tendon-like tissue was respectively 54.35% and 62.14% that of the contralateral (i.e., normal) Achilles tendons in the experimental group, and there was a significant difference detected between the experimental and normal Achilles tendons at two time points (both  $P < 0.001$ ). However, the maximum load of the experimental group was superior to that of the control group (50.78% and 51.87%, respectively), with a significant difference observed at 20 weeks post-operatively ( $P < 0.05$ ). At 10 and 20 weeks post-operatively, the maximum stress and elastic modulus of the neo-Achilles tendon-like tissue in the experimental group were superior to those in the control group, with significant differences observed at 20 weeks ( $P < 0.05$ ). The mechanical property was positively correlated with time in each group.

### 3.5. Quantitative RT-PCR detection of collagen I and III mRNA expression in the neo-Achilles tendon

In experimental group, collagen I mRNA expression was positive in the neo-Achilles tendon-like tissue at both 10 and 20 weeks post-operatively. However, collagen III expression was very weak at 10 weeks post-operatively and was negative at 20 weeks post-operatively. In control group, collagen I expression was positive at both 10 and 20 weeks post-operatively, but was weaker than that in the experimental group, and collagen III mRNA expression was negative at these two time points. Collagen III mRNA expression in the normal rabbit Achilles tendon tissue was also negative. Collagen I mRNA expression was initially low and then became high in both the experimental and control groups over time, but was still lower than that in the normal rabbit Achilles tendon tissue at both time points (Fig. 4).

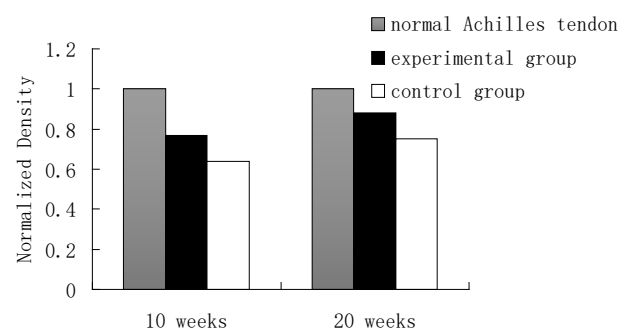


Fig. 4. Real-time quantitative RT-PCR analysis of collagen I mRNA expression in the neo-Achilles tendon. At 10 and 20 weeks post-operatively, collagen I mRNA expression was positive in the neo-Achilles tendon of rabbits in both experimental and control groups, but the expression in control group was weaker than that in experimental group. In experimental group and control group, collagen I mRNA expression increased with time, but was lower than that in the rabbit normal Achilles tendon. Collagen I mRNA expression in the rabbit normal Achilles tendon was set to 1 as a standard value



## 4. Discussion

With the development of materials science and biomedicine, transplantation of a tissue-engineered tendon is expected to become an ideal method to permanently cure tendon injury. Three-dimensional scaffolds constructed by tissue engineering of a biomaterial not only provide a favorable space for cells to gain nutrition, grow, and metabolize, but also provide structural support and act as a template to guide tissue regeneration and control the tissue structure. Cells seeded on a scaffold surface with porosity exhibit a higher survival rate and greater activity, which is favorable for cell proliferation and differentiation [23]. Therefore, in the research of tendon scaffold properties, in addition to consideration of the chemical and surface properties of a biomaterial, the structure of the three-dimensional scaffold should also be taken into account to facilitate cell adhesion and infiltration, nutrient delivery, and metabolic exchange. An increasing number of studies have focused on silk-based tissue engineering in recent years, which is considered an effective strategy for tendon reconstruction in a clinical setting [7]–[15], [24]–[26].

There are two main types of silk scaffolding: the first one based on a natural sericin-free silk fibroin fiber, which is woven into desirable shapes (e.g., rope-like, cable-like, braid-like) for tissue regeneration, and the other one, based on silk as a raw material, which is unglued, dissolved, filtered, dialyzed, and then processed into silk fibroin models of different forms. The most common type of regenerated silk fibroin biomaterial is a three-dimensional sponge-like silk fibroin scaffold, which can be fabricated by means of lyophilization and porosimetry. Importantly, its three-dimensional structure accurately mimics the three-dimensional structure of the body's physiological microenvironment, and the pore size of the scaffolds can be adjusted simply by using different freezing temperatures, solution pH values, and the amount of organic solution. Silk composite scaffolds are made of silk materials of different states, which improves their overall physical properties [27]–[29].

Porous silk fibroins containing microchannels and an aligned microfibril surface can increase the expression of tendon-specific extracellular matrix proteins along with the production of collagen, leading to the bundled growth of tendon cells, thereby contributing to the deposition of collagen. Therefore, the scaffold architecture plays an important role in the production of analogs and thus shows potential for the use in repairing damaged ligaments and tendons [30].

In the present study, we designed a weft-knitted mesh-like scaffold and the pores were filled with sponge-like regenerated silk fibroin/collagen to occupy the void space of the scaffold by means of reserved space. This created internal space could promote stromal production, generation of other cellular bioactive components, and further enhanced cell adhesion to the scaffold and cell affinity. Moreover, after implantation of the silk-based tissue-engineered tendons in an Achilles tendon defect rabbit model, no inflammatory cell infiltration was observed, and desirable histocompatibility was achieved. One important advantage of silk-based tissue-engineered tendons is their good similarity to biological tendons and the fact that they can be gradually substituted by autologous tendon tissue. Moreover, the use of weft-knitted silk fibroin fiber scaffolds overcomes the shortcoming of the excessively dense structure of a cable-like silk. The scaffolds incorporated with regenerated sponge-like fibroin/collagen further provide a mesh-like structure to enable cell ingrowth. Indeed, histological findings in the *in vivo* experiments showed that the weft-knitted silk fibroin fiber scaffolds allowed for the uniform distribution of cells, and promoted cell proliferation and differentiation. A collagen sponge can promote seed cell adhesion, and sponge-like regenerated fibroin/collagen can provide sufficient space for cell ingrowth. A knitted natural silk fiber scaffold can provide appropriate mechanical strength and its mechanical properties are more similar to those of normal tendon tissue, so that the tissue configuration and function effectively mimic those of the normal tendon tissue. In addition, this scaffold can promote the regeneration of neo-Achilles tendon through adjusting the secretion of extracellular matrix and the aggregation of collagen fibers, thereby facilitating the ingrowth of the surrounding tissue and ultimately promoting the repair of injured tendons.

Fibronectin-modified scaffolds have been shown to promote the growth of adherent cells and the secretion of matrix [31], [32]. Our preliminary experiments demonstrated that the BMSCs ran off easily on the non-modified scaffolds. However, after the scaffold surface was modified with fibronectin, cell adherence improved greatly. After 48 h of *in vitro* culture, scanning electron microscopy images showed that the BMSCs adhered to the scaffold surface and spread out, confirming that fibronectin-modified scaffolds greatly support the growth of BMSCs. Collagen contains RGD sequences at the adhesion site, which also enhance cell adherence. Repair of the Achilles tendon was also observed in control group to a certain degree. Twenty weeks after implantation, the knitted silk fiber

scaffolds without BMSCs generated some collagen I with a maximum load that was by 51.87% less than that of the natural Achilles tendon in rabbit. This suggests that the knitted silk fiber scaffold itself can guide tissue regeneration, which is an emerging research area in the field of biomaterials worldwide [33]–[35]. However, the weft-knitted silk scaffold incorporated with regenerated silk fibroin/collagen I and seeded with BMSCs further promoted the repair of rabbit Achilles tendons. Moreover, after implanting the scaffold–BMSCs composite into the gap deficits in the rabbit Achilles tendon, the composite retained excellent mechanical strength required by the body and kept the repaired Achilles tendons connected firmly at both ends. Twenty weeks after implantation, the scaffold–BMSCs composites showed good biocompatibility, and a tendon-like tissue was formed. Moreover, a large amount of uniform, neat, and dense collagen, mainly collagen I, was found in the neo-Achilles tendon. The new tendon tissue grew into the scaffold to form a “reinforced concrete”-like structure. The maximum load of the neo-Achilles tendon was improved compared to that of the control, at 62.14% that of the natural Achilles tendon. Therefore, based on the histological findings and mechanical function, the scaffold–BMSCs composites can promote the regeneration of tendon-like tissue, although this tissue is essentially different from the natural Achilles tendon. This suggests that tissue remodeling likely takes longer time and would occur under a more optimized condition. Therefore, selection of optimal seed cells, development of the optimal induction protocol, and the optimized combination of biomaterials should be further studied to enable clinical application of this tissue-engineered tendon for permanently repairing tendon injury.

## Acknowledgements

This research was supported by the Natural Science Foundation of Zhejiang Province of China, No. LY17H060011, LY17H280008, and LY18H180010; a grant from Zhejiang Provincial Medical Science and Technology Plan Project of China, No. 2015ZDA011, 2015KYB092, 2016KYB071, 2017KY303, and 2017KY307; a grant from Zhejiang Provincial Traditional Chinese Medicine Science and Technology Plan Project of China, No. 2015ZA045, 2016ZA044, and 2018ZA017; a grant from Zhejiang Provincial Science and Technology Plan Project of China, No. 2015C33109.

## References

- [1] BUTLER D.L., JUNCOSA N., DRESSLER M.R., *Functional efficacy of tendon repair processes*, *Annu. Rev. Biomed. Eng.*, 2004, 6, 303–329.
- [2] ABBAH S.A., SPANOUEDES K., O'BRIEN T., PANDIT A., ZEUGOLIS D.I., *Assessment of stem cell carriers for tendon tissue engineering in pre-clinical models*, *Stem. Cell. Res. Ther.*, 2014, 5(2), 38.
- [3] DOCHEVA D., MÜLLER S.A., MAJEWSKI M., EVANS C.H., *Biologics for tendon repair*, *Adv. Drug. Deliv. Rev.*, 2015, 84, 222–239.
- [4] SHARIFI-AGHDAM M., FARIDI-MAJIDI R., DERAKHSHAN M.A., CHEGENI A., AZAMI M., *Preparation of collagen/polyurethane/knitted silk as a composite scaffold for tendon tissue engineering*, *Proc. Inst. Mech. Eng. H.*, 2017, 231(7), 652–662.
- [5] YAO D., LIU H., FAN Y., *Silk scaffolds for musculoskeletal tissue engineering*, *Exp. Biol. Med.* (Maywood), 2016, 241(3), 238–245.
- [6] SHAPIRO E., GRANDE D., DRAKOS M., *Biologics in Achilles tendon healing and repair: a review*, *Curr. Rev. Musculoskelet. Med.*, 2015, 8(1), 9–17.
- [7] LIU H., FAN H., WANG Y., TOH S.L., GOH J.C., *The interaction between a combined knitted silk scaffold and microporous silk sponge with human mesenchymal stem cells for ligament tissue engineering*, *Biomaterials*, 2008, 29(6), 662–674.
- [8] LIU H., GE Z., WANG Y., TOH S.L., SUTTHIKHUM V., GOH J.C., *Modification of sericin-free silk fibers for ligament tissue engineering application*, *J. Biomed. Mater. Res. B Appl. Biomater.*, 2007, 82(1), 129–138.
- [9] ALTMAN G.H., DIAZ F., JAKUBA C., CALABRO T., HORAN R.L., CHEN J., LU H., RICHMOND J., KAPLAN D.L., *Silk-based biomaterials*, *Biomaterials*, 2003, 24(3), 401–416.
- [10] CAO Y., WANG B., *Biodegradation of silk biomaterials*, *Int. J. Mol. Sci.*, 2009, 10(4), 1514–1524.
- [11] GUO Y., CHEN Z., WEN J., JIA M., SHAO Z., ZHAO X., *A simple semi-quantitative approach studying the in vivo degradation of regenerated silk fibroin scaffolds with different pore sizes*, *Mater. Sci. Eng. C Mater. Biol. Appl.*, 2017, 79, 161–167.
- [12] ZUO BAOQI, WU ZHIYU, *Mechanical and biodegradable properties of regenerated fibroin fibers*, *Chinese Journal of Clinical Rehabilitation*, 2006, 10(1), 168–171.
- [13] ALTMAN G.H., HORAN R.L., LU H.H., MOREAU J., MARTIN I., RICHMOND J.C., KAPLAN D.L., *Silk matrix for tissue engineered anterior cruciate ligaments*, *Biomaterials*, 2002, 23(20), 4131–4141.
- [14] LI X., SNEDEKER J.G., *Wired silk architectures provide a biomimetic ACL tissue engineering scaffold*, *J. Mech. Behav. Biomed. Mater.*, 2013, 22, 30–40.
- [15] CHEN X., QI Y.Y., WANG L.L., YIN Z., YIN G.L., ZOU X.H., OUYANG H.W., *Ligament regeneration using a knitted silk scaffold combined with collagen matrix*, *Biomaterials*, 2008, 29(27), 3683–3692.
- [16] XU W., ZHOU F., OUYANG C., YE W., YAO M., XU B., *Mechanical properties of small-diameter polyurethane vascular grafts reinforced by weft-knitted tubular fabric*, *J. Biomed. Mater. Res. A*, 2010, 92(1), 1–8.
- [17] BUTLER D.L., JUNCOSA-MELVIN N., BOIVIN G.P., GALLOWAY M.T., SHEARN J.T., GOOCH C., AWAD H., *Functional tissue engineering for tendon repair: A multidisciplinary strategy using mesenchymal stem cells, bioscaffolds, and mechanical stimulation*, *J. Orthop. Res.*, 2008, 26(1), 1–9.
- [18] JUNCOSA-MELVIN N., BOIVIN G.P., GOOCH C., GALLOWAY M.T., WEST J.R., DUNN M.G., BUTLER D.L., *The effect of autologous mesenchymal stem cells on the biomechanics and histology of gel-collagen sponge constructs used for rabbit patellar tendon repair*, *Tissue Eng.*, 2006, 12(2), 369–379.

- [19] OUYANG H.W., GOH J.C., LEE E.H., *Viability of allogeneic bone marrow stromal cells following local delivery into patella tendon in rabbit model*, *Cell Transplant.*, 2004, 13(6), 649–657.
- [20] DAVIES B.M., MORREY M.E., MOUTHUY P.A., BABOLDASHTI N.Z., HAKIMI O., SNELLING S., PRICE A., CARR A., *Repairing damaged tendon and muscle: are mesenchymal stem cells and scaffolds the answer?* *Regen Med.*, 2013, 8(5), 613–630.
- [21] OUYANG H.W., GOH J.C., THAMBYAH A., TEOH S.H., LEE E.H., *Knitted poly-lactide-co-glycolide scaffold loaded with bone marrow stromal cells in repair and regeneration of rabbit Achilles tendon*, *Tissue Eng.*, 2003, 9(3), 431–439.
- [22] LIU H., FAN H., TOH S.L., GOH J.C., *A comparison of rabbit mesenchymal stem cells and anterior cruciate ligament fibroblasts responses on combined silk scaffolds*, *Biomaterials*, 2008, 29(10), 1443–1453.
- [23] CAMILO C.C., FORTULAN C.A., IKEGAMI R.A., SANTOS AR., DE M.P.B., *Manufacturing of porous alumina scaffolds with Bio-Glass and HAp coating: mechanical and In vitro evaluation*, *Key Engineering Materials*, 2009, 396–398, 679–682.
- [24] MANDAL B.B., KUNDU S.C., *Biospinning by silkworms: silk fiber matrices for tissue engineering applications*, *Acta Biomater.*, 2010, 6(2), 360–371.
- [25] SHARIFI-AGHDAM M., FARIDI-MAJIDI R., DERAKHSHAN M.A., CHEGENI A., AZAMI M., *Preparation of collagen/polyurethane/knitted silk as a composite scaffold for tendon tissue engineering*, *Proc. Inst. Mech. Eng. H*, 2017, 231(7), 652–662.
- [26] MUSSON D.S., NAOT D., CHHANA A., MATTHEWS B.G., MCINTOSH J.D., LIN S.T., CHOI A.J., CALLON K.E., DUNBAR P.R., LESAGE S., COLEMAN B., CORNISH J., *In vitro evaluation of a novel non-mulberry silk scaffold for use in tendon regeneration*, *Tissue Eng. Part A*, 2015, 21(9–10), 1539–1551.
- [27] KASOJU N., BORA U., *Silk fibroin in tissue engineering*, *Adv. Healthc. Mater.*, 2012, 1(4), 393–412.
- [28] ROCKWOOD D.N., PREDAR C., YÜCEL T., WANG X., LOVETT M.L., KAPLAN D.L., *Materials fabrication from Bombyx mori silk fibroin*, *Nat. Protoc.*, 2011, 6(10), 1612–1631.
- [29] VEPARI C., KAPLAN D.L., *Silk as a biomaterial*, *Prog. Polym. Sci.*, 2007, 32(8–9), 991–1007.
- [30] JAO D., MOU X., HU X., *Tissue regeneration: a silk road*, *J. Funct. Biomater.*, 2016, 7(3), 22.
- [31] LU H.H., COOPER J.A. JR, MANUEL S., FREEMAN J.W., ATTAWIA M.A., KO F.K., LAURENCIN C.T., *Anterior cruciate ligament regeneration using braided biodegradable scaffolds: in vitro optimization studies*, *Biomaterials*, 2005, 26(23), 4805–4816.
- [32] ATTIA M., SANTERRE J.P., KANDEL R.A., *The response of annulus fibrosus cell to fibronectin-coated nanofibrous polyurethane-anionic dihydroxyoligomer scaffolds*, *Biomaterials*, 2011, 32(2), 450–460.
- [33] SMEETS R., KNABE C., KOLK A., RHEINNECKER M., GRÖBE A., HEILAND M., ZEHBE R., SACHSE M., GROBE-SIESTRUP C., WÖLTJE M., HANKEN H., *Novel silk protein barrier membranes for guided bone regeneration*, *J. Biomed. Mater. Res. B Appl. Biomater.*, 2017, 105(8), 2603–2611.
- [34] OLIVEIRA A.L., SUN L., KIM H.J., HU X., RICE W., KLUGE J., REIS R.L., KAPLAN D.L., *Aligned silk-based 3-D architectures for contact guidance in tissue engineering*, *Acta Biomater.*, 2012, 8(4), 1530–1542.
- [35] MADDURI S., PAPALOİZOS M., GANDER B., *Tropically and topographically functionalized silk fibroin nerve conduits for guided peripheral nerve regeneration*, *Biomaterials*, 2010, 31(8), 2323–2334.